bio-protocol

Open Access

Published: Jun 20, 2025

An Optimized Ex Vivo Protocol for Quantitative Electrophysiological Assessment of Neuromuscular Junctions and Skeletal Muscle Function Using the Aurora System

Can Cui[1, 2, #, §], Zhengyuan Bao[3, #], Simon Kwoon-Ho Chow[4], Qianjin Wang[1, 2], Senlin Chai[1, 2], Zhihong Xu[3], Qing Jiang[3, *], Wing Hoi Cheung[1, 2, *]

[1]Musculoskeletal Research Laboratory, Department of Orthopaedics and Traumatology, Prince of Wales Hospital, The Chinese University of Hong Kong, Hong Kong SAR, China
[2]Li Ka Shing Institute of Health Sciences, The Chinese University of Hong Kong, Hong Kong SAR, China
[3]Division of Sports Medicine and Adult Reconstructive Surgery, Department of Orthopedic Surgery, Nanjing Drum Tower Hospital, Affiliated Hospital of Medical School, Nanjing University, Nanjing, Jiangsu, China
[4]Department of Orthopaedic Surgery, Stanford University, Stanford, CA, USA
*For correspondence: louischeung@cuhk.edu.hk
[#]Contributed equally to this work
[§]Technical contact: cancui@cuhk.edu.hk

Abstract

The neuromuscular junction (NMJ) is critical for muscle function, and its dysfunction underlies conditions such as sarcopenia and motor neuron diseases. Current protocols for assessing NMJ function often lack standardized stimulation parameters, limiting reproducibility. This study presents an optimized ex vivo method to evaluate skeletal muscle and NMJ function using the Aurora Scientific system, incorporating validated stimulation protocols for both nerve and muscle to ensure consistency. Key steps include tissue preparation in a low-calcium, high-magnesium solution to preserve NMJ integrity, determination of optimal muscle length, and sequential stimulation protocols to quantify neurotransmission failure and intratetanic fatigue. By integrating rigorous standardization, this approach enhances reproducibility and precision, providing a robust framework for investigating NMJ pathophysiology in aging and disease models.

Key features

- Dual stimulation modes enable direct muscle and indirect nerve stimulation to isolate NMJ-specific dysfunction.
- Optimized stimulation parameters for nerve (5 mA, 0.8 ms pulse width) and muscle (300 mA, 0.2 ms pulse width) on mouse model.
- Preservation of NMJ integrity through dissection in low-calcium, high-magnesium artificial cerebrospinal fluid (aCSF) and synthetic interstitial fluid (SIF).
- Quantitative analysis of neurotransmission failure and intratetanic fatigue using standardized equations.

Keywords: Ex vivo muscle function, Neuromuscular junction, Optimal stimulation parameters, Neurotransmission failure, Intratetanic fatigue, Sarcopenia models

This protocol is used in: Ageing Cell (2024), DOI: 10.1111/acel.14156

Graphical overview

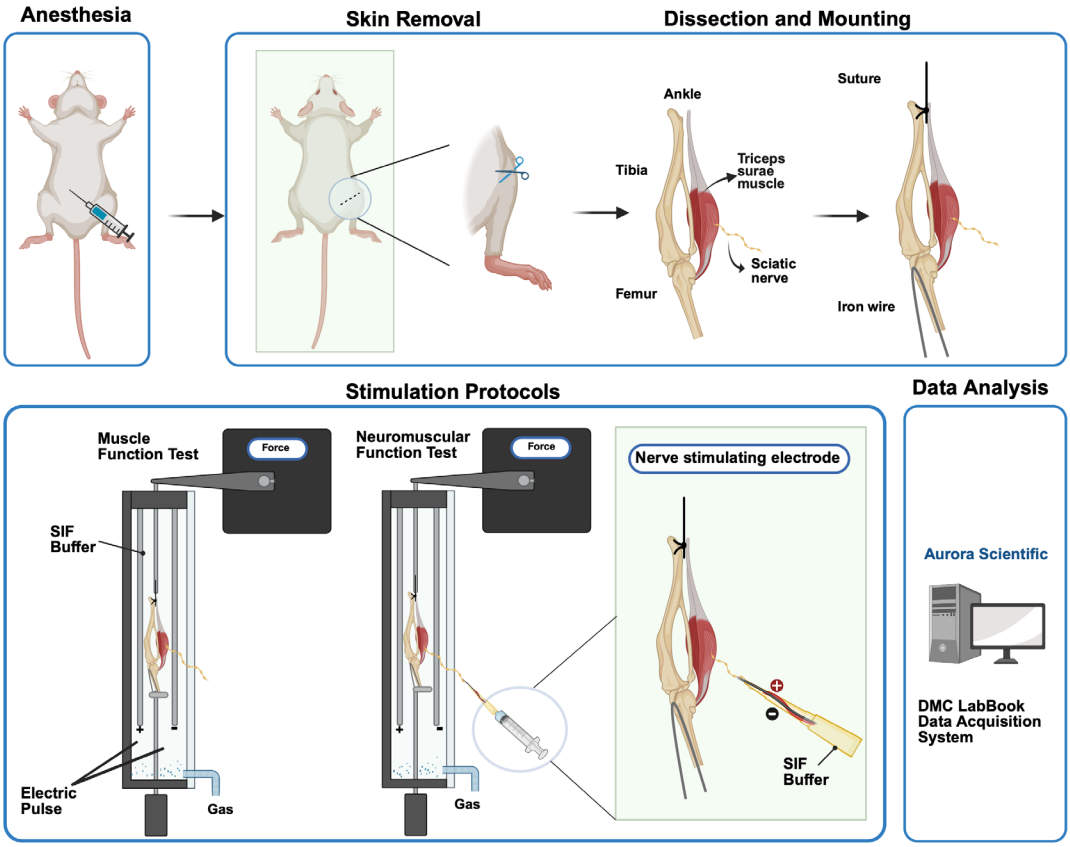

Steps to stimulate triceps surae–sciatic nerve to test muscle and neuromuscular junction (NMJ) function contraction: For tissue preparation, the triceps surae–sciatic nerve is dissected in a low-calcium, high-magnesium artificial cerebrospinal fluid (aCSF). Then, the preparation is transferred to the ex vivo system tank in synthetic interstitial fluid (SIF) perfused with mixed oxygen (95% oxygen, 5% carbon dioxide). Tendons are clamped to a force transducer (Aurora Scientific 800C-1, Newmarket, Canada) to measure isometric contractions. During stimulation, two parallel electrodes stimulate muscle contraction directly. The suction electrode induces muscle contraction indirectly by stimulating the sciatic nerve. Optimal muscle length (L_0) is determined by incrementally stretching the muscle until maximal twitch force is achieved, ensuring standardized sarcomere alignment. Twitch force (F_0) and tetanic force (F_t) of muscle and nerve are acquired by stimulating the muscle and sciatic nerve in a validated sequence. Results are recorded with the DMC LabBook data acquisition system (Aurora Scientific) and analyzed by the analysis system.

Background

The neuromuscular junction (NMJ), a specialized synapse bridging motor neurons and skeletal muscle fibers, is indispensable for voluntary movement and autonomic function. Its dysfunction underlies a spectrum of pathologies, including sarcopenia, amyotrophic lateral sclerosis (ALS), and myasthenic syndromes, which affect millions globally [1–3]. Traditional methodologies for assessing NMJ integrity and function have relied on in vivo electrophysiology, histological analyses, and electron microscopy (EM), which provide critical insights into synaptic ultrastructure [4,5]. Ex vivo systems, such as the Aurora Scientific apparatus, have emerged as powerful tools for isolating NMJ physiology by enabling direct muscle and indirect nerve stimulation [6]. Despite their utility, existing protocols exhibit critical limitations, notably inconsistent stimulation parameters (e.g., pulse width, frequency) and inadequate preservation of NMJ structure during tissue preparation, leading to interlaboratory variability and diminished reproducibility [7].

Recent studies employing ex vivo systems have underscored the importance of standardized parameters in quantifying

neurotransmission failure (NF) and intratetanic fatigue (IF), key metrics of NMJ resilience. For instance, Rizzuto et al. (2015) demonstrated that precise stimulation protocols are essential for detecting NMJ dysfunction in the SOD1(G93A) mouse model of amyotrophic lateral sclerosis (ALS), highlighting how variable pulse widths and frequencies can obscure synaptic deficits [7]. Similarly, Pratt et al. (2015) reported that inconsistent stimulation currents in dystrophic (mdx) mice led to misinterpretations of NMJ fatigue, emphasizing the need for protocol standardization [8]. Moreover, the use of non-physiological dissection buffers often compromises NMJ morphology [9]. Franco et al. (2014) revealed that conventional saline solutions accelerate synaptic vesicle depletion, compromising NMJ integrity [10]. This issue is particularly relevant in aging models, where NMJ morphology is already vulnerable. Recent work by Wang et al. (2023) further demonstrated that low-calcium, high-magnesium dissection buffers mitigate synaptic transmission inhibition, preserving NMJ architecture in murine sarcopenia models [11]. These technical shortcomings could impede translational research, leading to conflicting outcomes in therapeutic trials for neuromuscular disorders [12,13].

To address these challenges, this protocol introduces an optimized ex vivo framework that integrates (1) validated stimulation parameters for nerve (5 mA, 0.8 ms pulse width) and muscle (300 mA, 0.2 ms pulse width) to maximize activation fidelity; (2) a low-calcium, high-magnesium dissection buffer to preserve NMJ ultrastructure by inhibiting spontaneous neurotransmitter release [10]; and (3) standardized equations for quantifying NF and IF, enabling direct comparisons across experimental models. By coupling these advancements with the Aurora Scientific system's dual-mode lever and real-time data acquisition, this approach enhances precision in evaluating NMJ pathophysiology, as demonstrated in murine models of sarcopenia [14–16]. The protocol's reproducibility and translational relevance are further evidenced by its application in identifying NMJ-specific deficits in aging mice [17].

This methodological advancement bridges a critical gap in neuromuscular research and provides a platform for mechanistic studies of NMJ-targeted therapies. It could accelerate the development of interventions for conditions where synaptic failure precedes muscle atrophy, such as early-stage ALS or chemotherapy-induced neuropathy in the murine model [18].

Materials and reagents

Biological materials

1. C57BL/6, senescence accelerated mouse (SAMP8) and the age-matched control senescence-resistant inbred strains (SAMR1)

Reagents

1. Sodium pentobarbital (Alfasan, catalog number: 16582)
2. Sodium chloride (NaCl) (Thermofisher, catalog number: S/3160/65)
3. Potassium chloride (KCl) (Thermofisher, catalog number: P/4240/60)
4. Magnesium sulfate, heptahydrate ($MgSO_4·7H_2O$) (Sigma-Aldrich, catalog number: M1880)
5. Sodium bicarbonate ($NaHCO_3$) (Thermofisher, catalog number: 424270010)
6. HEPES (VWR, catalog number: 0511-250G)
7. Glucose (Sigma-Aldrich, catalog number: G8270)
8. Calcium chloride ($CaCl_2$) (Sigma-Aldrich, catalog number: 902179-1KG)
9. Sodium dihydrogen phosphate monohydrate ($NaH_2PO_4. H_2O$) (AlfaAesar™, catalog number: 115911)
10. Sodium gluconate ($NaC_6H_{11}O_7$) (ShangHai EKEAR Bio@Tech Co. LTD, catalog number: EC208-407-7)
11. Sucrose (Thermofisher, catalog number: BP220-1)
12. Potassium dihydrogen phosphate (KH_2PO_4) (VWR, catalog number: 26936.293)

Solutions

1. 1× Synthetic interstitial fluid (SIF) (see Recipes)
2. 1 × Artificial cerebrospinal fluid (aCSF) (see Recipes)

Recipes

1. 1× Synthetic interstitial fluid (SIF), pH 7.4 ± 0.05

Reagent	Final concentration	Quantity or Volume
NaCl	123 mM	7.188 g
KCl	3.5 mM	0.261 g
$MgSO_4·7H_2O$	0.7 mM	0.173 g
HEPES	10 mM	2.383 g
Glucose	5.5 mM	0.991 g
$CaCl_2$	2 mM	0.222 g
$NaH_2PO_4. H_2O$	1.7 mM	0.235 g
$NaC_6H_{11}O_7$	9.5 mM	1.160 g
Sucrose	7.5 mM	2.567 g
Total (optional)	n/a	1,000 mL

2. 1× Artificial cerebrospinal fluid (aCSF), pH 7.4 ± 0.05

Reagent	Final concentration	Quantity or Volume
NaCl	128 mM	7.480 g
KCl	1.9 mM	0.142 g
$MgSO_4·7H_2O$	6.5 mM	1.602 g
$NaHCO_3$	26 mM	2.184 g
Glucose	10 mM	1.802 g
$CaCl_2$	0.85 mM	0.094 g
KH_2PO_4	1.2 mM	0.163 g
Total (optional)	n/a	1,000 mL

Laboratory supplies

1. 5 mL disposable syringe (Terumo, catalog number: SS+10L)
2. 3-way stopcock (Taobao, Shengdakang company, catalog number: n/a)
3. Single strand ultra-fine soft high-temperature silver-plated wire (0.3 mm) (Taobao, Shanghai Haoyu tech company, catalog number: n/a)
4. Iron wire (0.3 mm) (Taobao, catalog number: n/a)
5. Mersilk braided silk suture 4-0 (Johnson & Johnson, catalog number: SA83G)
6. BNC to dual alligator clip oscilloscope probe test lead cable (1 m, 3 ft) (Taobao, catalog number: n/a)
7. 200 µL pipette tips (Multi, catalog number: 15730)
8. 90 × 20 mm cell culture dish (SPL Life Sciences, catalog number: 20100)

Equipment

A. Surgical tools (Figure 1)

1. Serrated forceps
2. Tian Gong ultra-fine microsurgical forceps (0.34 mm) (Taobao, catalog number: n/a)
3. Tian Gong microdissecting spring scissors (1.1 cm) (Taobao, catalog number: n/a)
4. Tian Gong premium gold-handled scissors (9.5cm) (Taobao, catalog number: ZHTG)
5. Metal robotic arm (Taobao, catalog number: n/a)

Figure 1. Surgical tools for sample preparation. From left to right, serrated forceps, ultra-fine microsurgical forceps, microdissecting spring scissors, gold-handled scissors, suture and wire are prepared for animal experiment.

B. Testing and recording equipment (Figure 2)

1. In-vitro Test Apparatus (Vertical, Aurora Scientific Inc., Newmarket, Canada, catalog number: 800C-1)
2. Dual-mode lever, stimulator (Aurora Scientific Inc., Newmarket, Canada, catalog number: 150A)
3. 5% CO_2/O_2 in compressed gas cylinder (Linde HKD Ltd)

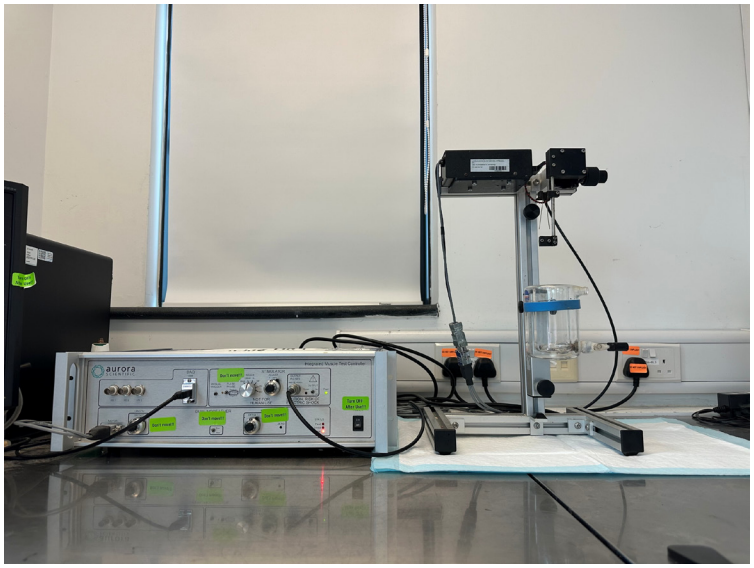

Figure 2. Ex vivo muscle functional test system. The system consists of the Dual-mode lever stimulator (left) and the In-vitro Test Apparatus (right).

Software and datasets

1. DMC LabBook data acquisition system (Aurora Scientific Inc, Newmarket, Canada, catalog number: 610A, version DMCV6.000)
2. Analysis system (Aurora Scientific Inc, Newmarket, Canada, catalog number: 615B, version DMAv5.501)

Procedure

A. Preparation of nerve-stimulating electrode

Based on the protocol of Johnson et al. [19], our group developed a simple stimulator with bent 200 μL pipette tips, a three-way stopcock, a syringe, and silver-plated wires for electric conduction (Figures 3–5).

1. Prepare the suction stimulator. First, cut the first 1/3 tip of the 200 μL pipette tips to create a 2.54 mm-diameter round suction nozzle. Then, melt and bend the neck of the 200 μL pipette tips to 60° and wait 1–2 min to mold (Figure 3B).
2. Drill a hole in the main body for the silver-plated wire to pass through.
3. Prepare two silver-plated wires for the electrode. With forceps, remove approximately 5 cm of wire insulation to expose the wires (Figure 3E).
4. Wrap one stripped wire around the insulation of the other wire to form the electrode (Figure 3F).
5. Pass the electrode through the hole of the pipette model and attach the other ends of the two wires to the lead cable (Figure 3G and Figure 4A).
6. Connect the suction electrode, 3-way stopcock, and syringe together to form the nerve-stimulating electrode (Figures 4B and 5). Wrap Parafilm around the suction electrode to ensure air tightness.
7. Connect the nerve-stimulating electrode to the metal robotic arm. Fix the arm on the operating table (Figure 6).

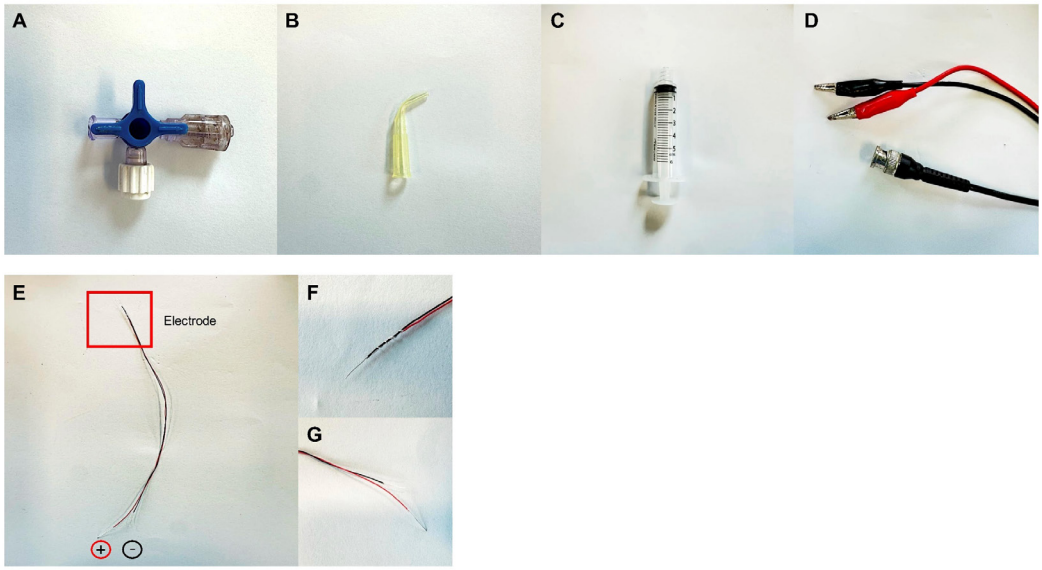

Figure 3. Components of the nerve-suction electrode. (A–D). The simulator is composed of a 3-way stopcock (A), pipette tip (B), a 5 mL syringe (C), and a BNC to dual alligator clip oscilloscope probe test lead cable (D). (E) Two silver-plated wires are tangled together (F) to form the electrode. (G) The other ends of the wires are exposed and then connected to the cable.

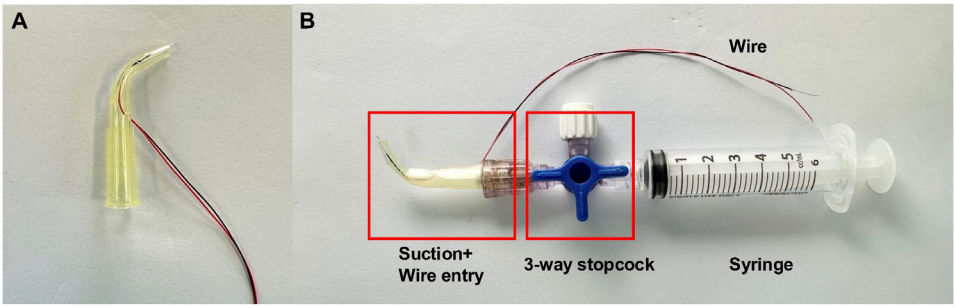

Figure 4. Construction of the nerve-stimulating electrode. (A) The wire electrode is passed through the hole of the pipette model. (B) Different components are connected to form the nerve suction electrode.

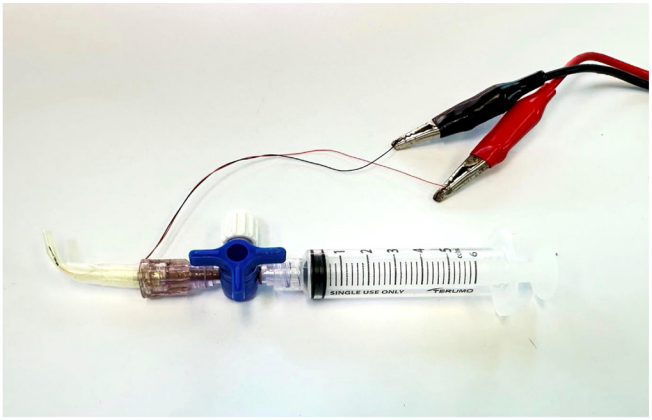

Figure 5. The nerve-stimulating electrode is connected to the lead cable. The lead cable will be attached to the ex vivo muscle functional test system during nerve stimulation.

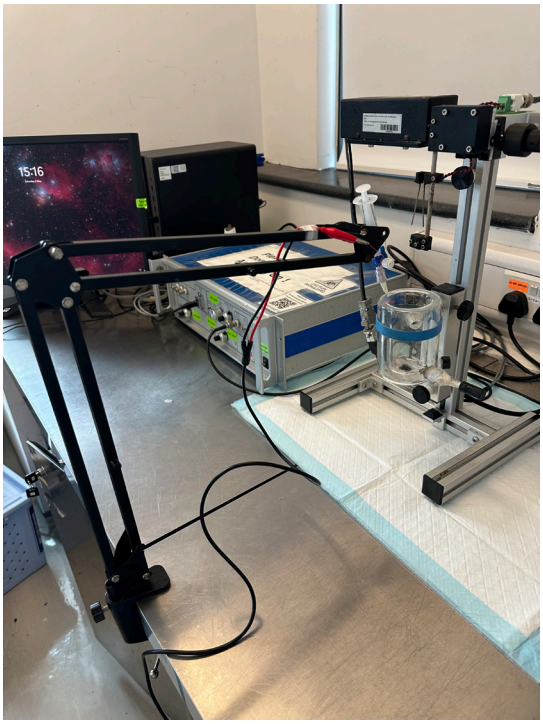

Figure 6. The nerve-stimulating electrode is connected to the metal robotic arm. The preparation section is complete.

B. Dissection and mounting

To preserve intact nerve terminals and NMJ structure to the greatest extent, the triceps surae–sciatic nerve is used to test muscle and NMJ function. The triceps surae is a muscle group composed of the gastrocnemius and the soleus, which plays an important role in maintaining posture and body movement. Refer to Video 1 for the detailed dissection and mounting procedures. Video time stamps of individual steps are provided in the text.

1. Administer sodium pentobarbital (1.5 mg/mouse, intraperitoneal) for sustained anesthesia (Video 1, 00:00–00:08).

Critical: Monitor breathing closely to prevent an overdose. Parameters include monitoring respiratory rate (steady, around 180 breaths per minute), observing chest movements for shallow or deep breathing, and any respiratory distress (irregular rhythms, gasping, or agonal breathing).

2. Remove the skin covering the right hindlimb (Figure 7A–B and Video 1, 00:09–00:37).

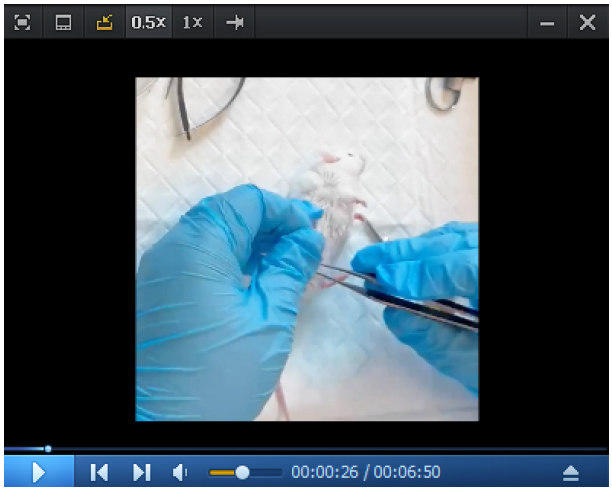

Video 1. Dissection and mounting procedures of the triceps surae–sciatic nerve. (00:00–00:08) Anesthesia. (00:09–00:37) Remove the skin covering the right hindlimb. (00:38–01:37) Remove tibialis anterior (TA), extensor digitorum longus (EDL), and quadriceps. (01:38–01:52) Isolate the triceps surae–Achilles' tendon complex and tie the tendon with braided silk suture. (01:53–03:12) Expose sciatic nerve. (03:13–03:18) Cut the Achilles' tendon with distal tibia and femur condyle. (03:19–05:33) Complete isolation of triceps surae–sciatic nerve in aCSF buffer. (05:34–06:16) Cross iron wire through femur cavity. (06:17–06:35) Place mounted tissue sample in ex vivo system tank. (06:36–end) Suck the floating sciatic nerve into the nerve stimulator electrode.

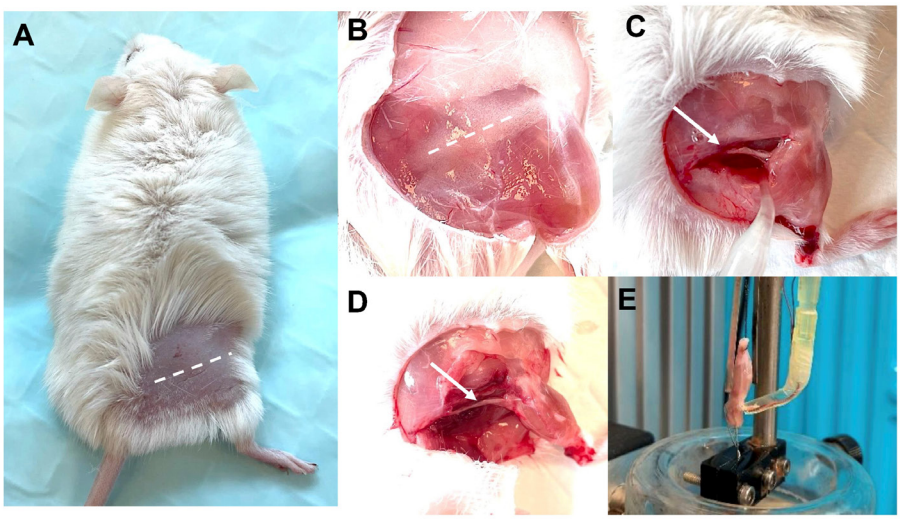

Figure 7. Exposure and isolation of the triceps surae–sciatic nerve. (A–B) The skin covering the hindlimb is removed to expose the sciatic nerve. (C–D) The incision is made in the upper and lateral part of the leg along the femur, and other connecting tissues are removed to expose the triceps surae and sciatic nerve. (E) After mounting, the preparation is equilibrated to room temperature (22–25 °C) in oxygenated SIF solution for 10 min prior to experiment. The sample is fixed on the ex vivo functional system.

3. Remove tibialis anterior (TA), extensor digitorum longus (EDL), and quadriceps muscles (Video 1, 00:38–01:37).
4. Isolate the triceps surae–Achilles' tendon complex and tie the tendon with braided silk suture (Video 1, 01:38–01:52).
5. Expose the sciatic nerve. Remove all connecting tissue around the sciatic nerve (Figure 7C–D and Video 1, 01:53–03:12).
6. Cut the Achilles' tendon together with the distal tibial and sciatic nerve, as well as the femur condyle (Video 1, 03:13–03:18).
7. Immediately place the sample in the cell culture dish with chilled low calcium, high magnesium aCSF solution (Video 1, 03:19–05:33), which can inhibit synaptic transmission during the dissection of surrounding soft tissues [10].

Caution: aCSF buffer must be kept ice-cold.

8. With the knee joint bending, cross an iron wire through the femur pulp cavity until the condylar nest and joint capsule are penetrated (Video 1, 05:34–06:16).
9. Place the mounted tissue sample in the ex vivo system tank in SIF perfused with mixed oxygen (95% oxygen, 5% carbon dioxide) (Video 1, 06:17–06:35) [10].
Caution: After mounting, the preparation is equilibrated to room temperature (22–25°C) in oxygenated SIF solution for 10 minutes prior to the next experiment.
10. Fix the femur cavity to the ex vivo machine with a hook using the iron wire.
11. Pass the braided silk suture through the hole of the transducer's lever arm to grasp the Achilles' tendon and allow the muscle to equilibrate in the solution.
12. Tie the muscle vertically between the two electrodes, which can directly stimulate muscle contraction (Figure 7E).
13. Suck the floating sciatic nerve into the nerve stimulating electrode, which can induce muscle contraction indirectly (Video 1, 06:36–end). The sciatic nerve is parallel to the electrode and keeps floating in the suction nozzle.
Caution: Handle with extreme care to prevent any damage to the sciatic nerve during the procedure.

C. Stimulation protocols (Figures 8–10)

1. Measure optimal length (L0) by eliciting isometric twitch while gradually increasing muscle length until maximal force is generated (300 mA, 0.2 ms pulse width).
2. Twitch force (F_0) measurements: Stimulate the muscle with a single square pulse [stimulus intensity 300 mA, stimulus width 0.2 ms (Twitch M)] once and the nerve with a single squire pulse [stimulus intensity 5 mA, stimulus width 0.8 ms pulse width (Twitch N)] once with a 1 min interval.
Caution: After twitch force, there is a 1-min interval to the subsequent tetanic force measurement.
3. Tetanic force (Ft) measurements: Apply one direct stimulation from the two parallel electrodes on the ex vivo system (300 mA, 300 ms duration, 0.2 ms pulse width, 50 Hz stimulation frequency, Tetanic M) to the muscle once and then one stimulation from the nerve suction stimulator on the nerve (5 mA, 300 ms duration, 0.8 ms pulse width, 50 Hz stimulation frequency, Tetanic N) once with 2 min intervals.
Caution: After twitch force, there is a 2-min interval to the following fatigue assessment.
4. Fatigue assessment:
(1) Fatigue via nerve (Fatigue N): Perform 100 cycles of 50 Hz tetanic stimulation (0.7 s rest between cycles) via the sciatic nerve.
Caution: After the first fatigue sequence, there is a 15-min interval to the second fatigue sequence.
(2) Fatigue via muscle (Fatigue M): Perform 100 cycles of 50 Hz tetanic stimulation (0.7 s rest between cycles) directly on the muscle.
5. Gently take down the muscle after the sequence is finished and measure the wet muscle weight on a balance.

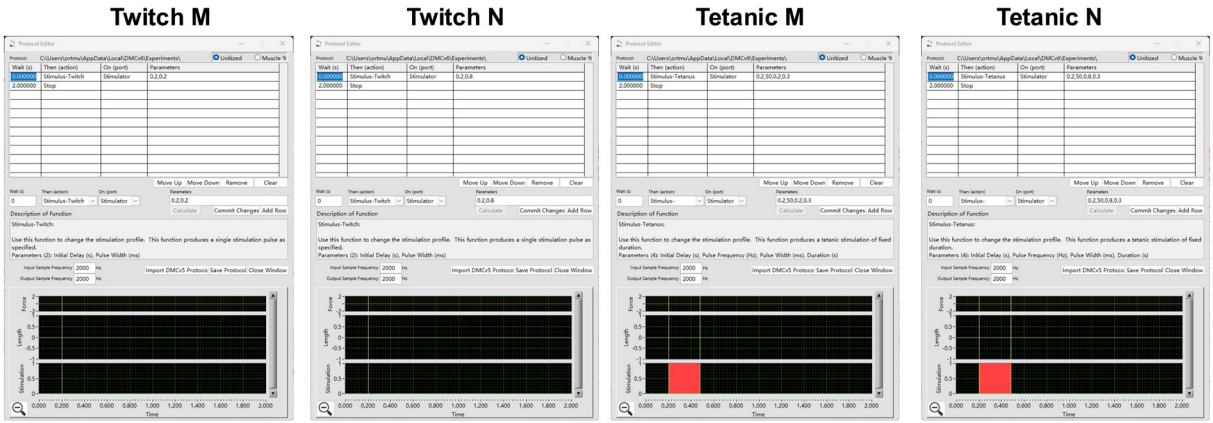

Figure 8. Ex vivo skeletal muscle and neuromuscular junction (NMJ) functional test protocol. Protocols include Twitch M, Twitch N, Tetanic M, and Tetanic N stimulation, edited by DMC LabBook data acquisition system (Aurora Scientific).

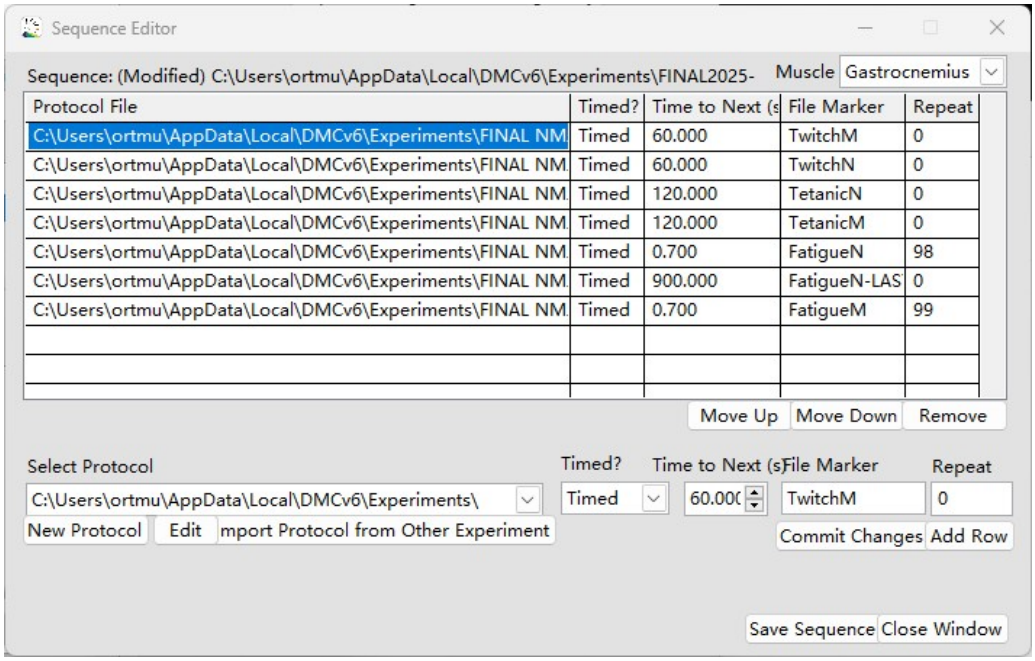

Figure 9. Ex vivo skeletal muscle and neuromuscular junction (NMJ) functional test sequence. The sequence is composed of Twitch M, Twitch N, Tetanic M, and Tetanic N protocols, edited by DMC LabBook data acquisition system (Aurora Scientific).

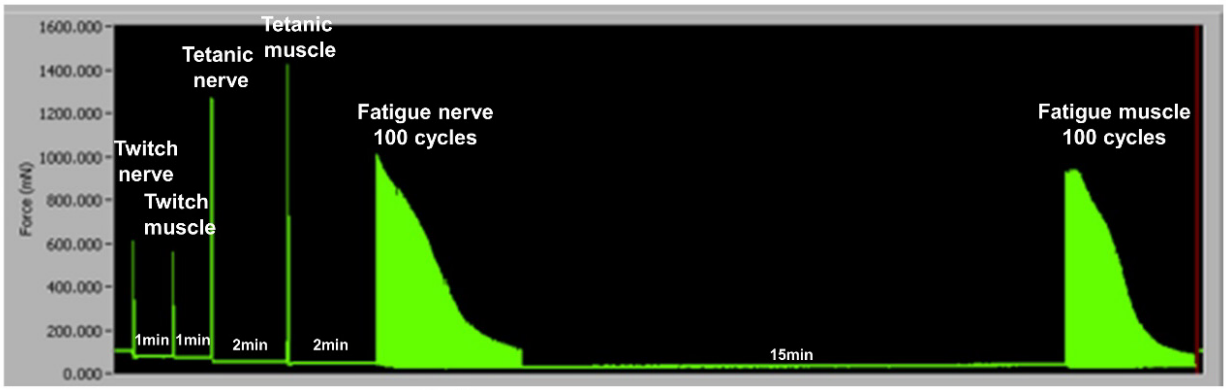

Figure 10. Ex vivo skeletal muscle and neuromuscular junction (NMJ) functional test diagram. Screenshot of the whole Ex vivo sequence, including Twitch N, Twitch M, Tetanic N, Tetanic M, Fatigue N and Fatigue M.

Data analysis

Results are recorded with the DMC LabBook data acquisition system (Aurora Scientific) and analyzed with the analysis system (Aurora Scientific).

1. Open the analysis system and choose *High Throughput* > *Force-Frequency Analysis* (Figure 11).

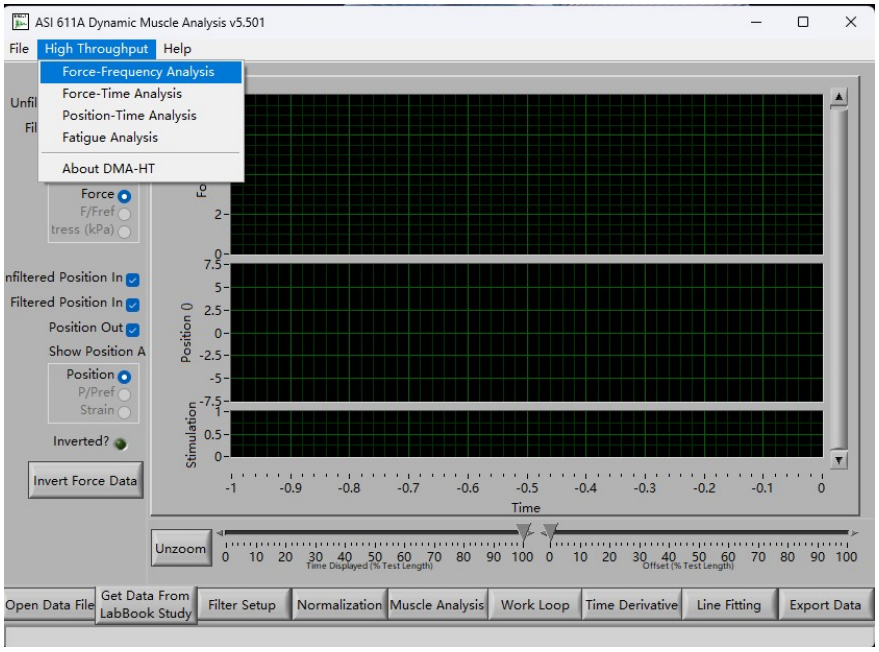

Figure 11. Main page of the analysis system

2. In the *High Throughput-Force-Frequency* page, choose *Manual* mode, and then change *Start Cursor* to 0.2 and *End Cursor* to 1.5. (Figure 12).

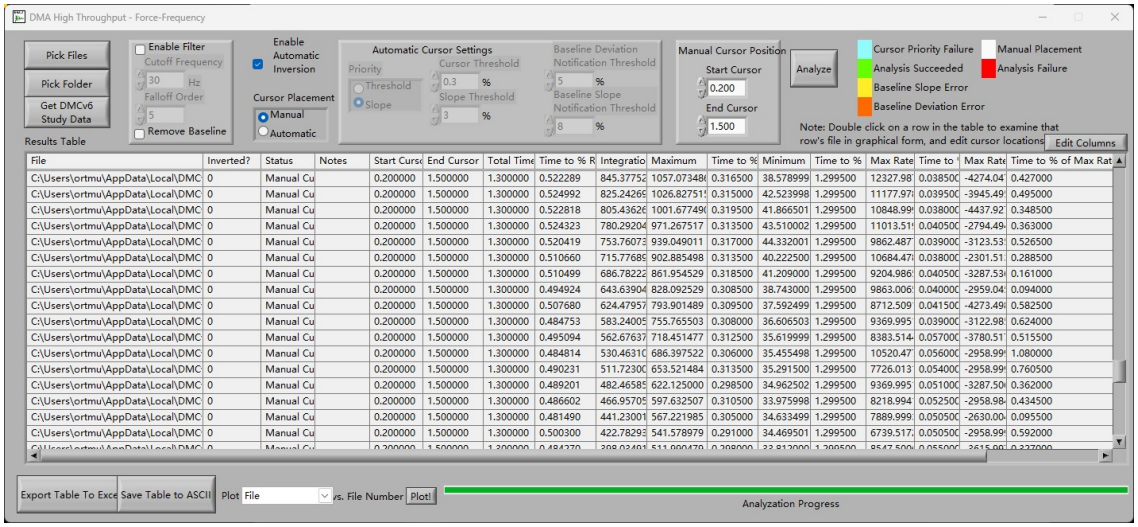

Figure 12. Analysis page of the system

3. Import all data to the *High Throughput-Force-Frequency* page, click on *Analyze*, and export the values to Excel for further analysis.

4. Force is calculated as Maximum minus Minimum.

5. Neurotransmission failure (NF) quantifies the progressive loss of muscle contraction force during repeated nerve stimulation, reflecting impaired transmission at the NMJ. It is expressed as the percentage decline in force relative to the initial contraction amplitude. Intratetanic fatigue (IF) measures the percentage decline in muscle force during a continuous train of high-frequency stimulation. It evaluates NMJ-dependent fatigue (via nerve stimulation) and muscle-specific fatigue (via direct muscle stimulation).

(1) F means percent force decline during nerve stimulation.

$$\mathrm{F}\ (\%) = \left(1 - \frac{\text{Force at nth stimulus}}{\text{Initial Force}}\right) \times 100$$

Initial force: Peak force during the first 10 stimuli.
Force at nth stimulus: Peak force at specific intervals (e.g., 50th, 100th stimulus).

(2) MF means percent force decline during muscle stimulation:

$$\mathrm{MF}\ (\%) = \left(1 - \frac{\text{Force at nth stimulus}}{\text{Initial Force}}\right) \times 100$$

Initial force: Peak force during the first 10 stimuli.
Force at nth stimulus: Peak force at specific intervals (e.g., 50th, 100th stimulus).

(3) The NF and IF are calculated according to the following equations:

$$NF = \frac{\mathrm{F} - \mathrm{MF}}{1 - MF}\%$$
$$IF = \frac{F_{lp}}{F_m}\%$$

F: percent force loss during nerve stimulation;
MF: percent force loss during muscle stimulation;
Flp: force generated at the last pulse of stimulation;
Fm: the maximum force generated during the same pulse train.

6. Normalize force by muscle cross-sectional area (MCSA).
Normalized by MCSA, the specific twitch force (SF_0) and specific tetanic force (SF_t) are obtained. The MCSA, SF_0, and SF_t are calculated according to the following equations.
CSA is calculated by dividing the wet weight of triceps surae muscle by L0 and the density of mammalian skeletal muscle (1.06 mg/mm^3).

$$MCSA\ (mm^2) = \frac{MM\ (mg)}{\left(\frac{L}{L_0}\right) \times D \times L_0(mm)}$$
$$SF_0(mN/mm^2) = \frac{F_0\ (mN)}{MCSA\ (mm^2)}$$
$$SF_t(mN/mm^2) = \frac{F_t\ (mN)}{MCSA\ (mm^2)}$$

D = Muscle density = 1.06 mg/mm^3
MM = Muscle mass (mg)
L/L0 is the fiber-to-muscle length ratio. The triceps surae muscle was the sole target of this project, so L/L0 = 1 was set to simplify the calculation.

Validation of protocol

This protocol was validated by Bao et al. [17], demonstrating consistent NMJ dysfunction in sarcopenic mice. SAMP8 at 6 months old were used to confirm the optimum parameter values. Three different frequencies were tried to trigger triceps surae contraction. 50 Hz was found optimal to induce the maximal contraction by stimulating the muscle and sciatic nerve. At 80 Hz of nerve stimulation, there was an obvious slope at the platform of the oscillograph, indicating this frequency was too high in nerve tetanic stimulation. As a result, 50 Hz was determined as the optimum frequency of stimulation (Figure 13). To confirm the optimal stimulation current value, 100, 300, and 1,000 mA were used to induce triceps surae contraction

by directly stimulating the muscle, and 300 mA was found appropriate to trigger the maximal contraction. Therefore, 300 mA was determined as the optimum current to stimulate the muscle directly (Figure 13C). 1, 5, 10, and 100 mA were applied to induce triceps surae contraction by stimulating the sciatic nerve, and 5 mA was able to trigger the maximum muscle contraction. Hence, 5 mA was determined as the optimum current to stimulate the sciatic nerve (Figure 13D). To confirm the optimal stimulation pulse width, 0.2, 0.5, 0.8, and 1.0 ms were used to induce triceps surae twitch contraction by directly stimulating the muscle or the sciatic nerve. Then, to better protect NMJ function during muscle stimulations, we chose 0.2 ms as the optimum pulse width for muscle. Furthermore, to fully activate NMJ and observe NMJ functional differences more easily, we chose 0.8 ms as the optimum pulse width for nerve (Figure 13E).

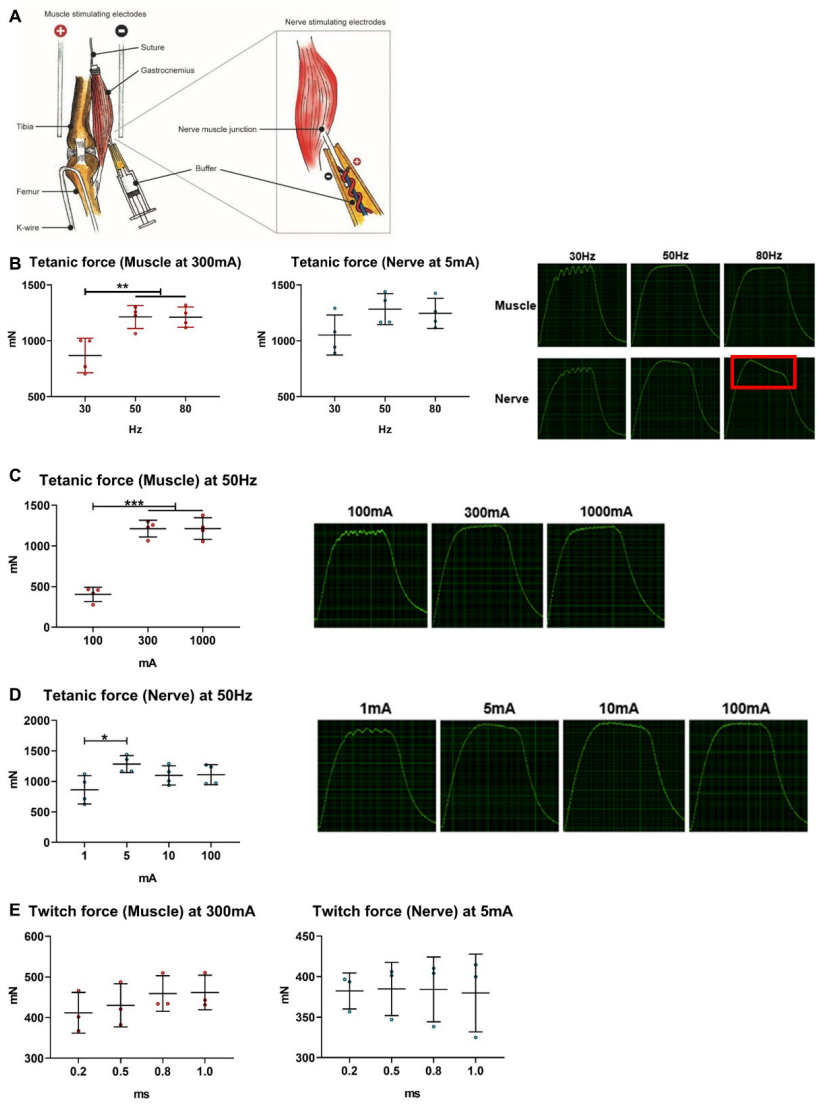

Figure 13. Validating the optimal stimulation frequency and current intensity in ex vivo neuromuscular junction (NMJ) and muscle function test. (A) Apparatus to assess ex vivo NMJ and muscle function test. Two parallel electrodes could stimulate muscle contraction directly. The suction electrode could induce muscle contraction indirectly by stimulating the sciatic nerve. (B) 50 Hz was optimal to induce the maximal contraction by stimulating the muscle and the sciatic nerve; a significant slope at the platform was observed in the oscillograph of nerve stimulation at 80 Hz (n = 4). (C) 300 mA was sufficient to trigger the maximal contraction by directly stimulating the muscle, and no obvious differences in the platform in the oscillograph were observed between 300 and 1,000 mA of muscle stimulations (n = 4). (D) 5 mA was sufficient to trigger the maximum muscle contraction by stimulating the sciatic nerve, and no obvious differences in the platform in the oscillograph were observed among 5, 10, and 1,000 mA of nerve stimulations (n = 4). (E) In twitch stimulation, no significant difference of twitch force was observed between 0.2, 0.5, 0.8, and 1.0 ms of pulse width by stimulating the muscle or sciatic nerve (n = 3). * $p < 0.05$, ** $p < 0.01$, *** $p < 0.001$ in Bonferroni post-hoc test following one-way ANOVA.

General notes and troubleshooting

General notes

1. The protocol was established on C57BL/6J, SAMP8, and SAMR1 mice; tetanic stimulations of muscle and nerve may need to be altered for different strains. To adjust the protocol, we could start with low currents (e.g., 1–2 mA) and incrementally increase until supramaximal response is achieved (all fibers recruited). We could also adjust pulse width (ms) to sufficiently excite muscle and nerve.

Troubleshooting

Problem: Low force output during nerve stimulation (tetanic value below 200 mN).
Possible cause: Damaged NMJ due to improper dissection.
Solution: Ensure tissue remains in a low-calcium solution during dissection.

Problem: Excessive muscle fatigue during high-frequency fatigue stimulation (>80% decline in force).
Possible cause: Inadequate oxygenation of SIF.
Solution: Maintain 95% O_2/5% CO_2 perfusion.

For a force range, please kindly refer to the forces of SAMP8 mice at different timepoints (Table 1; mean ± SD). Data was published in Bao et al. [17].

Table 1. Force range of SAMP8 mice at 3, 6, 8, 10, and 12-month-old. Data are shown as mean ± SD.

SAMP8	Twitch M (mN)	Twitch N (mN)	Tetanic M (mN)	Tetanic N (mN)
3-month-old	454.29 ± 63.93	384.92 ± 44.67	1,064.41 ± 130.04	949.92 ± 109.03
6-month-old	413.65 ± 37.77	403.58 ± 44.91	1,172.61 ± 119.47	1,013.35 ± 113.40
8-month-old	521.79 ± 64.82	525.03 ± 68.73	1,342.97 ± 83.28	1,257.52 ± 128.13
10-month-old	470.32 ± 62.03	443.65 ± 84.53	1,119.12 ± 172.16	1,036.05 ± 131.6
12-month-old	425.54 ± 46.22	436.59 ± 56.82	998.02 ± 61.26	1,002.87 ± 125.89

Acknowledgments

Author contributions: C.C. and Z.Y.B. conceived the idea, designed the project, and performed all experiments. W.H.C., Z.H.X. and Q.J. obtained the funding. S.K.-H.C., C.S.L., and Q.J.W. helped with the experiments and gave input to data analysis. C.C. and C.S.L. took the video, and C.C. edited the footage and figures. C.C. drafted the protocol, Z.Y.B. and W.H.C. revised the manuscript, and C.C. finished it.

This work was supported by Collaborative Research Fund (Ref: C4032–21GF), General Research Grant (Ref: 14114822), Group Research Scheme (Ref: 3110146), Health Care and Promotion Scheme (Ref: 02180118), Area of Excellence (Ref: AoE/M-- 402/20), National Basic Research Program of China (Ref: 2021YFA1201404), Science and Technology Cooperation Program (Ref: 202308002), and Major Project of NSFC (Ref: 81991514). The protocols described here are adapted from our previous work [17].

Competing interests

The authors have declared that no conflict of interest exists.

Ethical considerations

The animal subjects involved in this protocol were obtained from the Laboratory Animal Service Center at the Chinese University of Hong Kong. The research protocol was approved by the Animal Experimentation Ethics Committee of the Chinese University of Hong Kong (Ref: 18/262/MIS).

Received: March 17, 2025; Accepted: May 22, 2025; Available online: June 10, 2025; Published: June 20, 2025

References

1. Arnold, W. D. and Clark, B. C. (2023). Neuromuscular junction transmission failure in aging and sarcopenia: The nexus of the neurological and muscular systems. *Ageing Res Rev.* 89: 101966. https://doi.org/10.1016/j.arr.2023.101966
2. Chen, L. K., Woo, J., Assantachai, P., Auyeung, T. W., Chou, M. Y., Iijima, K., Jang, H. C., Kang, L., Kim, M., Kim, S., et al. (2020). Asian Working Group for Sarcopenia: 2019 Consensus Update on Sarcopenia Diagnosis and Treatment. *J Am Med Dir Assoc.* 21(3): 300–307.e2. https://doi.org/10.1016/j.jamda.2019.12.012
3. Valdez, G., Tapia, J. C., Lichtman, J. W., Fox, M. A. and Sanes, J. R. (2012). Shared Resistance to Aging and ALS in Neuromuscular Junctions of Specific Muscles. *PLoS One.* 7(4): e34640. https://doi.org/10.1371/journal.pone.0034640
4. Willadt, S., Nash, M. and Slater, C. R. (2016). Age-related fragmentation of the motor endplate is not associated with impaired neuromuscular transmission in the mouse diaphragm. *Sci Rep.* 6(1): p24849. https://doi.org/10.1038/srep24849
5. Jones, R. A., Reich, C. D., Dissanayake, K. N., Kristmundsdottir, F., Findlater, G. S., Ribchester, R. R., Simmen, M. W. and Gillingwater, T. H. (2016). NMJ-morph reveals principal components of synaptic morphology influencing structure–function relationships at the neuromuscular junction. *Open Biol.* 6(12): 160240. https://doi.org/10.1098/rsob.160240
6. Pratt, S. J. P., Shah, S. B., Ward, C. W., Kerr, J. P., Stains, J. P. and Lovering, R. M. (2014). Recovery of altered neuromuscular junction morphology and muscle function in mdx mice after injury. *Cell Mol Life Sci.* 72(1): 153–164. https://doi.org/10.1007/s00018-014-1663-7
7. Rizzuto, E., Pisu, S., Musarò, A. and Del Prete, Z. (2015). Measuring Neuromuscular Junction Functionality in the SOD1G93A Animal Model of Amyotrophic Lateral Sclerosis. *Ann Biomed Eng.* 43(9): 2196–2206. https://doi.org/10.1007/s10439-015-1259-x
8. Hughes, S., Jagannath, A., Hickey, D., Gatti, S., Wood, M., Peirson, S. N., Foster, R. G. and Hankins, M. W. (2014). Using siRNA to define functional interactions between melanopsin and multiple G Protein partners. *Cell Mol Life Sci.* 72(1): 165–179. https://doi.org/10.1007/s00018-014-1664-6
9. Murray, L., Gillingwater, T. H. and Kothary, R. (2014). Dissection of the *Transversus Abdominis* Muscle for Whole-mount Neuromuscular Junction Analysis. *J Vis Exp.* 2014(83): p. e51162. https://doi.org/10.3791/51162
10. Franco, J. A., Kloefkorn, H. E., Hochman, S. and Wilkinson, K. A. (2014). An In Vitro Adult Mouse Muscle-nerve Preparation for Studying the Firing Properties of Muscle Afferents. *J Vis Exp.* 2014(91): p. 51948. https://doi.org/10.3791/51948-v
11. Wang, C., Zhao, B., Zhai, J., Wang, A., Cao, N., Liao, T., Su, R., He, L., Li, Y., Pei, X., et al. (2023). Clinical-grade human umbilical cord-derived mesenchymal stem cells improved skeletal muscle dysfunction in age-associated sarcopenia mice. *Cell Death Dis.* 14(5): p321. https://doi.org/10.1038/s41419-023-05843-8
12. Kiernan, M. C., Vucic, S., Talbot, K., McDermott, C. J., Hardiman, O., Shefner, J. M., Al-Chalabi, A., Huynh, W., Cudkowicz, M., Talman, P., et al. (2020). Improving clinical trial outcomes in amyotrophic lateral sclerosis. *Nat Rev Neurol.* 17(2): 104–118. https://doi.org/10.1038/s41582-020-00434-z
13. Tintignac, L. A., Brenner, H. R. and Rüegg, M. A. (2015). Mechanisms Regulating Neuromuscular Junction Development and Function and Causes of Muscle Wasting. *Physiol Rev.* 95(3): 809–852. https://doi.org/10.1152/physrev.00033.2014
14. Guo, A. y., Leung, K. s., Qin, J. h., Chow, S. h. and Cheung, W. h. (2016). Effect of Low-Magnitude, High-Frequency Vibration Treatment on Retardation of Sarcopenia: Senescence-Accelerated Mouse-P8 Model. *Rejuvenation Res.* 19(4): 293–302. https://doi.org/10.1089/rej.2015.1759

15. Bao, Z., Cui, C., Chow, S. H., Qin, L., Wong, R. M. Y. and Cheung, W. H. (2020). AChRs Degeneration at NMJ in Aging-Associated Sarcopenia–A Systematic Review. *Front Aging Neurosci.* 12: e597811. https://doi.org/10.3389/fnagi.2020.597811
16. Cui, C., Bao, Z., Chow, S. H., Wong, R. M. Y., Welch, A., Qin, L. and Cheung, W. H. (2022). Coapplication of Magnesium Supplementation and Vibration Modulate Macrophage Polarization to Attenuate Sarcopenic Muscle Atrophy through PI3K/Akt/mTOR Signaling Pathway. *Int J Mol Sci.* 23(21): 12944. https://doi.org/10.3390/ijms232112944
17. Bao, Z., Cui, C., Liu, C., Long, Y., Wong, R. M. Y., Chai, S., Qin, L., Rubin, C., Yip, B. H. K., Xu, Z., et al. (2024). Prevention of age-related neuromuscular junction degeneration in sarcopenia by low-magnitude high-frequency vibration. *Aging Cell.* 23(7): e14156. https://doi.org/10.1111/acel.14156
18. Staff, N. P., Grisold, A., Grisold, W. and Windebank, A. J. (2017). Chemotherapy-induced peripheral neuropathy: A current review. *Ann Neurol.* 81(6): 772–781. https://doi.org/10.1002/ana.24951
19. Johnson, B. R., Hauptman, S. A., and Bonow, R. H. (2007). Construction of a simple suction electrode for extracellular recording and stimulation. *J Undergrad Neurosci Educ.* 6(1): p. A21-6. https://pubmed.ncbi.nlm.nih.gov/23493751/